MEASUREMENT OF RF LOSSES DUE TO TRAPPED FLUX IN A LARGE-GRAIN NIOBIUM CAVITY*

G. Ciovati#, Jefferson Lab, Newport News, VA 23606, USA
A. Gurevich, NHMFL, Florida State University, Tallahassee FL 32310, USA

Abstract

Trapped magnetic field in superconducting niobium is a well known cause of radio-frequency (RF) residual losses. In this contribution, we present the results of RF tests on a single-cell cavity made of high-purity large grain niobium before and after allowing a fraction of the Earth magnetic field to be trapped in the cavity during the cooldown below the critical temperature T_c. This experiment has been done on the cavity before and after a low temperature baking. Temperature mapping allowed us to determine the location of hot-spots with high losses and to measure their field dependence. The results show not only an increase of the low-field residual resistance, but also a larger increase of the surface resistance for intermediate RF field (higher "medium field Q-slope"), which depends on the amount of the trapped flux. These additional field-dependent losses can be described as losses of pinned vortices oscillating under the applied RF magnetic field.

INTRODUCTION

Magnetic field trapped in niobium during cool-down across T_c is a well-known source of residual losses in superconducting RF cavities [1]. Earlier studies showed a linear increase of the residual losses with the trapped DC magnetic field [2-4]. In addition it was found that vortices result in a linear dependence of the surface resistance with the RF field and that this term also increases linearly with the trapped DC field, more strongly in Nb films sputtered on Cu than in bulk Nb cavities [5, 6]. In this study we use a thermometry system to detect, for the first time, "hot-spots" caused by frozen-in flux. We did these experiments on a large-grain single-cell after post-purification, low-temperature baking and buffered chemical processing to observe the difference in RF losses induced by vortices and to compare them to the losses which cause the high-field Q-drop.

EXPERIMENTAL SETUP AND RESULTS

The cavity used in this study is a large-grain single-cell cavity of the CEBAF shape (1.5 GHz) fabricated from Ningxia high purity (RRR>200) niobium. The cavity had been used for a previous study on oxidation published in Ref. [7]. A detailed description of the standard cavity preparation for a high-power RF test is also given in [7].

* This manuscript has been authored by Jefferson Science Associates, LLC under U.S. DOE Contract No. DE-AC05-06OR23177. The U.S. Government retains a non-exclusive, paid-up, irrevocable, world-wide license to publish or reproduce this manuscript for U.S. Government purposes.
#gciovati@jlab.org

A temperature mapping system, described in [8], consisting of 576 thermometers distributed on the outer cavity surface (1-2 cm spacing) allows measuring the local temperature rise due to RF losses. The Earth magnetic field is shielded in the cryostat where the cavity is tested to about 1-2 mG by a combination of μ-metal cylinder and a compensation coil wrapped around it, as shown schematically in Fig. 1. After a baseline RF test, the cavity is warmed up to about 15 K and the current in the compensation coil is changed, increasing the residual DC magnetic field in the cryostat. Following a cool down to 1.7 K, a high power RF test of the cavity is performed and, after warming-up and removing the cavity test stand from the cryostat, the DC magnetic field is measured with a gaussmeter. The field homogeneity over the cavity volume is about 10% and the direction is about 3° from the cavity axis.

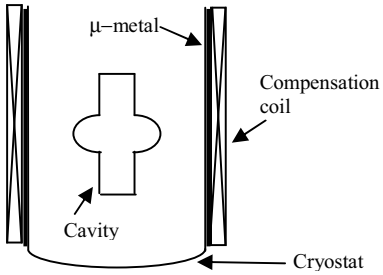

Figure 1: Schematic of magnetic shielding around the vertical cryostat for cavity testing.

During each RF test, the temperature dependence of the surface resistance at low field R_{s0} (B_p ~ 10 mT) is measured and fitted with the following Eq. (1) to obtain the residual resistance R^0_{res}:

$$R_{s0}(T) = R_{BCS}(T) + R^0_{res} \quad (1)$$

where $R_{BCS}(T)$ is the BCS surface resistance.

The first RF test was done after post-purification of the cavity at 1250 °C in a Ti box, followed by about 55 μm buffered chemical polishing (BCP) with HF, HNO_3 and H_3PO_4 in 1:1:1 ratio. The cavity was limited by high-field Q-drop with no field emission to a peak surface magnetic field B_p = 130 mT. The temperature maps showed few hot-spots in the equator region (Fig. 2a). The cavity was tested again after field cooling in 380 mG, R^0_{res} increased by 54.5 nΩ and the temperature maps showed additional hot-spots, mostly at the equator (Fig. 2b).

The cavity was then baked in ultra-high vacuum (UHV) at 120 °C for a total of 9 h and was tested again at 1.7 K. The limit was a quench at B_p = 169 mT, with no field emission. The Q-drop was eliminated and temperature maps showed a modest, uniform heating at the equator

(Fig. 2c). After field cooling in 264 mG, R^0_{res} increased by 39.8 nΩ and additional losses were measured by temperature mapping (Fig. 2d).

The cavity was then subjected to various cycles of low-temperature baking in different atmospheres and heat treatments at 600 °C, which will be discussed in a future publication. The cavity surface was then refreshed by etching a layer of about 17 µm with BCP 1:1:1 and the RF test at 1.7 K showed high-field Q-drop up to B_p = 129 mT (no field emission) and few hot-spots in the equator area (Fig. 2e). After field cooling in 295 mG, R^0_{res} increased by 74.0 nΩ and temperature maps revealed several hot-spots distributed uniformly in the cavity surface (Fig. 2f).

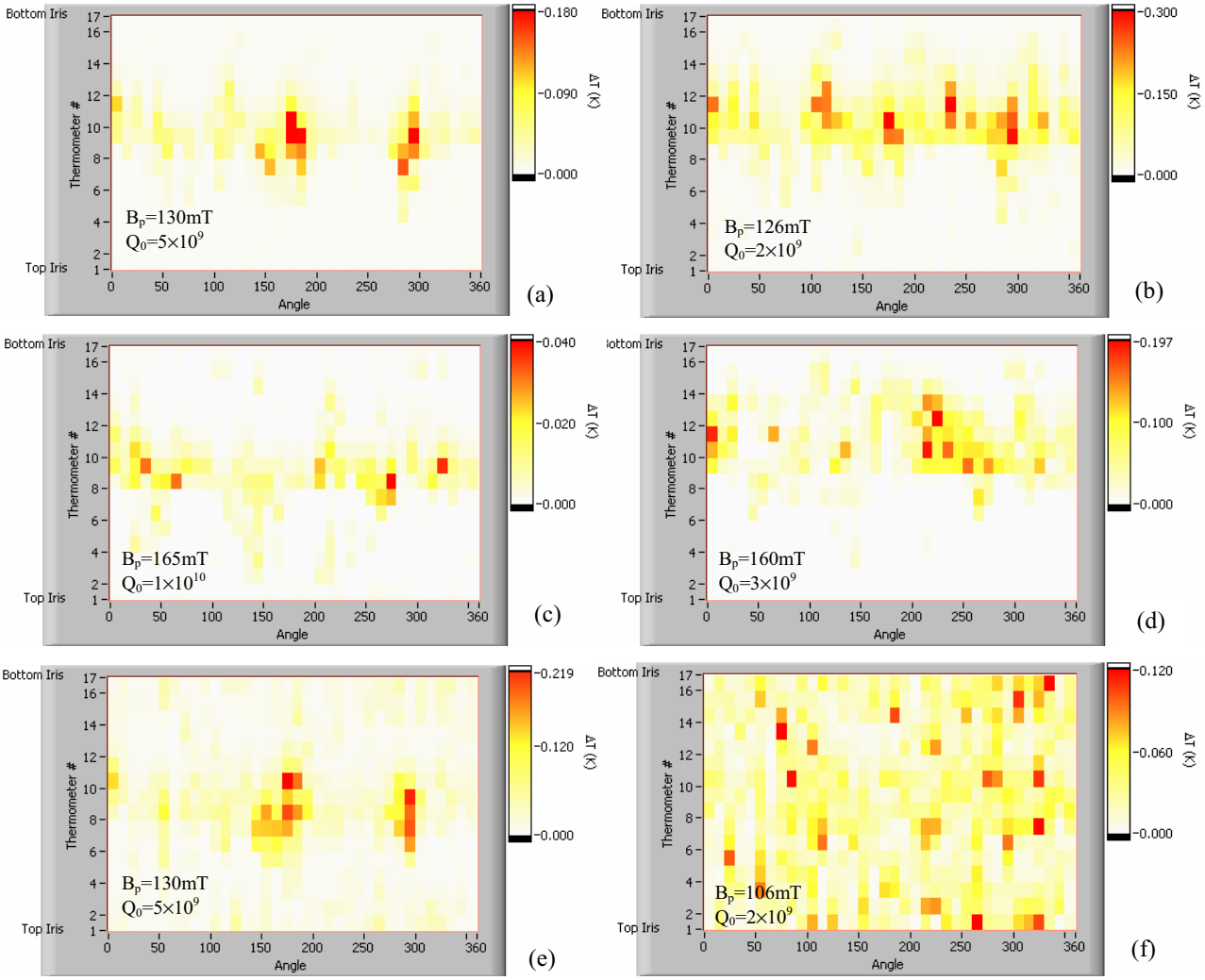

Figure 2: Temperature maps at the highest field reached during high-power RF test after post-purification at 1250 °C and 55 µm BCP 1:1:1 (a), after field cooling in 380 mG (b), after UHV baking at 120 °C for 9 h (c), after field cooling in 264 mG (d), after various heat treatments and 17 µm BCP 1:1:1 (e) and after field cooling in 295 mG. The He bath temperature is 1.7 K

DATA ANALYSIS

The field dependence of the surface resistance from 15 to 100 mT (medium field Q-slope) has been fitted by:

$$R_s\left(B_p\right) = R^1_{res} B_p + R_{s0}\left[1+\gamma\left(\frac{B_p}{B_c}\right)^2\right] \qquad (2)$$

which was used to analyze the results from several Nb cavities with different crystallographic structure [9]. B_c is the critical field at 0 K, assumed to be 200 mT, γ is a coefficient describing the overheating of the cavity surface with respect to the He bath [10] and intrinsic non-linearities of R_{BCS} [11]. R^1_{res} may be related to hysteresis losses due to "strong-links" created at Nb surfaces by oxidation [9]. It was shown that trapped vortices result in the additional surface resistance R_{fl} described by [5]

$$R_{fl} = \left(R^0_{fl} + R^1_{fl} B_p\right) B_{ext} \qquad (3)$$

where B_{ext} is the trapped DC field. Here the term R^0_{fl} corresponds to the part of the residual resistance independent of the RF field, while R^1_{fl} account for the

linear term R^1_{res}. Our experimental results are well described by Eqs. (2, 3) in which the coefficient γ was about 0.7, independent of B_{ext}, while the linear term increased with B_{ext}. The values of R^0_{res}, R^1_{res}, R^0_{fl} and R^1_{fl} for the various treatments are shown in Table 1. The dependence of the vortex-induced losses on the RF field is shown in Fig. 3 for the test after post-purification.

Table 1: Values of R^0_{res}, R^1_{res}, R^0_{fl} and R^1_{fl} obtained from a fit of $R_s(T)$ and $R_s(B_p)$ with Eqs. (2, 3) and value of .the local losses exponent n of Eq. (4) averaged over several fluxon-induced hot-spots.

Cavity treatment	R^0_{res} (nΩ)	R^1_{res} (nΩ/mT)	R^0_{fl} (nΩ/G)	R^1_{fl} (nΩ/mT/G)	n
1250 °C post-purif.	6.5 ± 0.4	(3.5 ± 3.0)×10^{-3}	143 ± 12	0.48 ± 0.05	3.01 ± 0.01
120 °C/9 h UHV bake	10.2 ± 0.2	(3.6 ± 0.4)×10^{-2}	151 ± 12	0.35 ± 0.09	3.46 ± 0.01
BCP 1:1:1	8.0 ± 0.3	(2.3 ± 0.1)×10^{-2}	251 ± 20	0.55 ± 0.06	2.538 ± 0.004

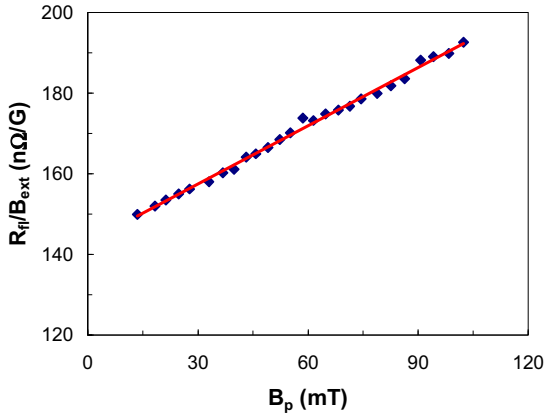

Figure 3: RF field dependence of the fluxon-induced losses at 1.7 K normalized to the trapped DC magnetic field for the test after post-purification at 1250 °C.

To gain more understanding of the mechanism of RF losses due to pinned vortices, it is useful to analyze the local temperature rise, ΔT, proportional to the local dissipated power, P, as a function of the RF field. Our data can be well described by the power law dependence:

$$\Delta T \propto P \propto B_p^n \qquad (4)$$

A typical plot of $log_{10}(\Delta T)$ vs. $log_{10}(B_p)$ for a hot-spot caused by a pinned vortex and for a hot-spot causing the high-field Q-drop is shown in Fig. 4. The value of n averaged over about 10 hot-spots due to trapped flux is shown in Table 1 and is different for the various cavity treatments, possibly indicating different physical mechanisms, as it will be discussed in the next section.

Figure 5 shows the heating at the same hot-spot on the cavity equator which contributes to the high-field Q-drop with and without trapped flux. The stronger heating already occurring at low field, suggests the presence of trapped vortices at this location.

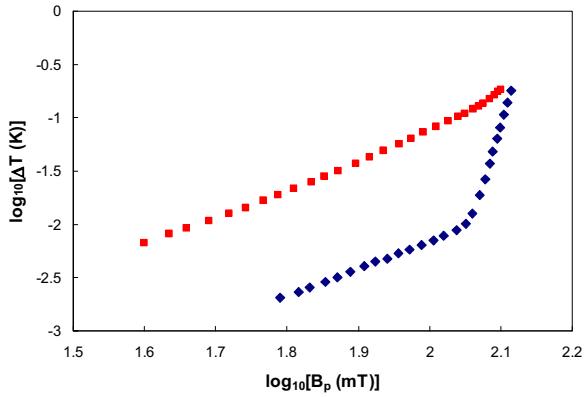

Figure 4: Field dependence of the local heating at a hot-spot caused by trapped vortices (red squares) and at a hot-spot causing the high-field Q-drop (blue diamonds).

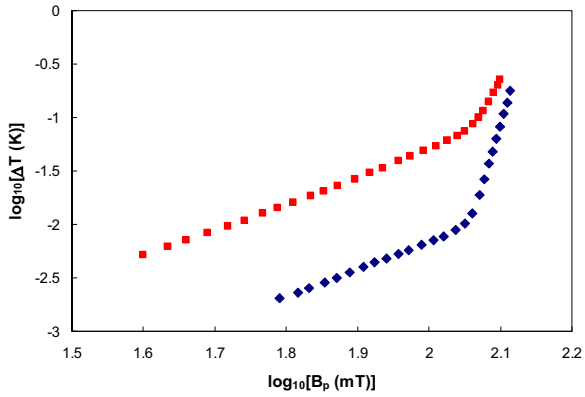

Figure 5: Field dependence of the local heating at the same hot-spot causing the high-field Q-drop (blue diamonds) and after field cooling (red squares).

DISCUSSION

The experimental results show that after the cavity was subjected to various heat treatments, baking and BCP, there is a significantly higher sensitivity of the residual

resistance to trapped flux, R^0_{fl}, an increased number of hot-spots and a different field dependence of the losses, compared to the cavity after post-purification with Ti at 1250 °C for several hours. This suggests a reduced trapping efficiency in annealed Nb, due to decrease of the density of pinning centers consistent with magnetization measurements done on Nb samples [12]. The value of R^0_{fl} reported in Table 1 for the post-purified cavity is in very good agreement with previous values reported in Ref. [3, 5] for an annealed cavity, where it was also reported a partial flux trapping, measured with Hall probes near the cavity surface. R^0_{fl} = 250 nΩ/G was measured on a heat treated cavity in [4]. In [13] a higher value of R^0_{fl} (350 nΩ/G) was reported for a Nb cavity, with no specification of the treatment, and a 100% trapping efficiency was measured on Nb plates. Our results confirm that R^0_{fl} in Nb depends on the state of the material. The values of R^1_{fl} in Table 1 are also in good agreement with the one in [5]. Detailed studies of R^0_{fl} and R^0_{fl} in sputtered Nb/Cu films, showed that R^0_{fl} can be one order of magnitude lower than bulk Nb, while R^1_{fl} can be more than one order of magnitude higher than bulk Nb, causing a much stronger medium field Q-slope. It was found that the nature of the noble gas used in the sputtering discharge and the nature of the interface between the film and the substrate were the main factors determining the values of R^0_{fl} and R^1_{fl}. These factors influence the pinning strength, which affects the intensity of the RF losses. A model describing the dynamics of vortex penetration and dissipation in RF fields was recently developed [14]. In this model, the additional surface resistance due to trapped vortices oscillating around their equilibrium position due to the RF field was calculated. The results showed that:

- R^0_{fl} increases significantly as the superconductor gets dirtier.
- R^0_{fl} depends strongly on the size ℓ of pinned vortex segments.
- R^0_{fl} depends strongly on the relaxation time constant of the pinned vortex, τ_p.

In the case of sparsely spaced vortices at $\omega\tau_p < 1$ (ω is the RF angular frequency), R^0_{fl} was estimated to be [14]:

$$R^0_{fl} = \frac{(\omega\tau_p)^2}{30}\frac{\rho_n B_{ext}}{\lambda B_{c2}} \propto \ell^4 \rho_n \qquad (5)$$

where ρ_n is the normal-state resistivity, λ is the London penetration depth and B_{c2} is the upper critical field. The simplified Eq. (5) already describes the essential dependencies of R^0_{fl} on the pinning strength, the purity of the material, and the amount of trapped flux observed in our experiments.

The fraction of hot-spots due to trapped flux which occur within 1 cm from a grain boundary in the large-grain cavity used for our experiments was about 43%-53%. Positions and strengths of these vortex hotspots may be determined not only by the distribution of impurities and pinning centers in the material and by the applied dc field, but also by the distribution of significant thermoelectric currents generated by thermal gradients during the cavity cool down through the critical temperature. Thermoelectric currents may generate trapped vortices even in the absence of the dc field. The contribution of vortices on grain boundaries to the surface resistance can be two-fold. First, the boundaries not aligned with the RF field could locally reduce the magnetic surface barrier and thus serve as preferential places for penetration of the Abrikosov vortices [14]. However, the places of the cavity where the grain boundaries turn out to be parallel to the RF field manifest themselves as stronger hotspots with lower RF field onsets of vortex penetration. Here the RF dissipation can result from oscillations of either the Josephson vortices along weakly coupled boundaries or the mixed Abrikosov-Josephson vortices along strongly coupled boundaries [15]. The expansion of the vortex core under strong RF driving force can result in the field dependence of the surface resistance similar to that in Eq. (3). Thus, cavity treatments such as post-purification, baking and chemical etching can influence the behavior of vortices, most likely due to changes in the distribution of pinning centers and/or impurities in the material, as it was already argued in [9]. In turn, the RF dissipation due to trapped vortices at hotspots where the high-field Q-drop develops indicates the presence of "defects" which may lower the surface barrier and facilitate the penetration of vortices driven by strong RF-fields.

CONCLUSIONS

The experimental results on RF losses due to trapped vortices in a large-grain Nb cavity presented in this contribution show that:

- The state of the material has a significant influence on the flux trapping efficiency, and therefore on the sensitivity of the residual resistance to the external DC magnetic field during field cooling.
- The average RF losses increase linearly with increasing RF field, as it was observed in Nb films, although at a much lower rate than in cavities made of Nb films on Cu. In the latter case more trapped vortices might be generated by the Peltier thermopower at the Cu/Nb interface during the cavity cooldown below T_c.
- Different dependencies of the local dissipated power as a function of the RF field for different surface conditions suggest changes in vortex type and dynamics.
- It is possible that the high-field Q-drop may be due to vortices penetrating the Nb surface at locations of reduced surface barrier under strong RF fields.

REFERENCES

[1] H. Padamsee, J. Knobloch and T. Hays, "RF superconductivity for accelerators", J. Wiley & Sons, New York, 1998.

[2] B. Piosczyk et al., IEEE Trans. Nucl. Sci. 20 (1973) 108.

[3] G. Arnold-Meyer and W. Weingarten, IEEE Trans. Magn. 23 No. 2 (1987) 1620.
[4] P. Kneisel and B. Lewis, "Additional RF Surface Resistance in Superconducting Niobium Cavities Caused by Trapped Magnetic Flux", JLAB Tech Note 94-028 (1994).
[5] C. Benvenuti et al., "Magnetic Flux Trapping in Superconducting Niobium", 8th SRF Workshop, Abano Terme, October 1997, p. 331.
[6] S. Calatroni et al., Physica C 351 (2001) 429.
[7] G. Ciovati, P. Kneisel and A. Gurevich, Phys. Rev. STAB 10 (2007) 062002.
[8] G. Ciovati et al., "Temperature Mapping System for Single Cell Cavities", JLAB Tech Note 05-059 (2005).
[9] G. Ciovati and J. Halbritter, Physica C 441 (2006) 57.
[10] J. Halbritter, "Rf Residual Losses, High Electric and Magnetic rf Fields in Superconducting Cavities", 38th Eloisatron Workshop, Erice, 1999, p. 9.
[11] A. Gurevich, Physica C 441 No. 1-2 (2006) 38.
[12] M. Bahte, F. Herrmann and P. Schmüser, "Magnetization and Susceptibility Measurements on Niobium Samples for Cavity Production, 8th SRF Workshop, Abano Terme, October 1997, p. 881.
[13] C. Vallet et al., "Flux Trapping in Superconducting Cavities", EPAC '92, Berlin, 1992, p.1295.
[14] A. Gurevich and G. Ciovati, submitted to Phys. Rev. B (2007).
[15] A. Gurevich, Phys. Rev. B 65 (2002) 214531.